MEMS 1041

Semester Project

Design and Testing of a Breath Force Meter

Date:
11/20/2020

Professor:
Dr. John Whitefoot

Submitted By:
Frank Czura
Ashley Zagari

1. Abstract

During the COVID-19 pandemic, it is important to monitor the severity of symptoms of the virus in patients and watch for the emergence of symptoms in other individuals at risk of exposure. Using techniques developed throughout the MEMS 1041 course, including strain gauge theory, data acquisition, and signal conditioning techniques, a breath force meter capable of measuring peak breath force and lung capacity was constructed, tested, and analyzed using uncertainty analysis. After using iterative design methods, a stainless-steel beam of elastic modulus 180 [GPa], length 107.5 [mm] from the center of pressure to the center of the strain gauge, width 25.52 [mm], and height 0.39 [mm], was selected. The beam should in theory produce 44.0 [$\mu strain$] at the gauge for the minimum breath force, and 180. [$\mu strain$] at the gauge for the maximum breath force. The beam was then mounted to a PVC pipe and the entire setup was mounted to the table to conduct calibration, yielding a static sensitivity estimation of -16.8 [V/N]. Once calibration was complete, a hand pump was used to simulate breaths for a total of ten trials by connecting one end to the PVC pipe and measuring was recorded during the course of the simulated exhale. The results of the measurements yielded on average a 2.37 [L] measured volume; representing a 39.4% overestimation of the nominal volume used during testing of 1.70 [L]. Additionally, all measured forces and strains were significantly less than that expected in theory. Effective improvements to our design would include a predetermined volume flowrate for testing, offset null balancing for the amplifiers, the use of a shorter beam, and improved measurement techniques.

2. Theory

2.1. Beam Design and Beam Theory Used for Strain Gage Placement

A breath force meter is to be constructed using a cantilever beam mounted to a breathing tube and by measuring the strain at a strain gauge. The strain can be directly related to the force experienced by the beam at any point in time, and this can in turn be used to measure the peak force, average force, and total volumetric flow of air from a person's lungs. The purpose of this tool is to allow an individual to monitor their lung capacity during the COVID-19 pandemic that dramatically affects the respiratory systems of patients with the disease.

The basic design of the breath force meter is shown in Figure 1. The plate (located at the right most side of the tube) resists the user's breath flow and creates a stagnation pressure, which is directly related to the measurement of strain and force described above. A half-inch diameter PVC pipe (with an internal diameter of 15.2 [mm]) will serve as the tube for this device.

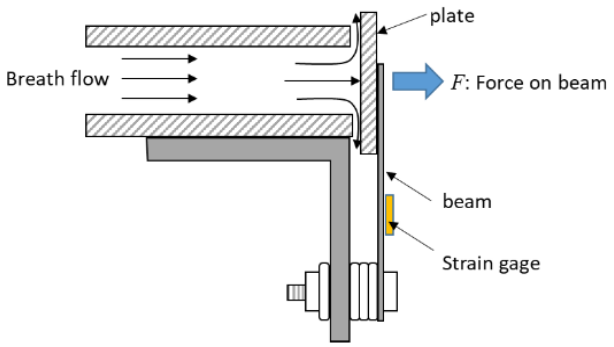

Figure 1: Design of Breath Force Meter (Reproduced from MEMS 1041 Semester Project Description with permission of the MEMS Dept., University of Pittsburgh)

On average, a full exhale can range anywhere from 0.9-1.3 [s], and adult human lung capacity is ranges from 5-7 [L] of air [1]. Logically, the most forceful breath would be the greatest lung capacity exhaled in the shortest time, and conversely the least forceful breath would be the least lung capacity exhaled in the longest time. The temperature and pressure inside the lungs are slightly above atmospheric, but it is reasonable to assume that the fluid being measured is air at atmospheric conditions flowing in a laminar fashion.

With the assumptions given above, the mass flowrate for the maximum and minimum force conditions can be calculated as follows:

$$\dot{m} = \rho \dot{\forall} = \rho \frac{\forall}{t} \tag{1}$$

where ρ is the density of air at atmospheric conditions (taken to be 1.169 $\left[\frac{kg}{m^3}\right]$), $\forall$ is the total volume present in the lungs in $[m^3]$, and t is the time taken for a full exhale, in [s]. Additionally, the flow velocity $\vec{V}$ can be computed via the following equation:

$$\vec{V} = \frac{\dot{\forall}}{A_{CS}} \tag{2}$$

where $\dot{\forall}$ is the volumetric flowrate in $\left[\frac{m^3}{s}\right]$ and A_{CS} is the cross-sectional area of the inside of the PVC pipe (taken to be $1.81\ x\ 10^{-4}[m^2]$ given the above inner diameter). To obtain a value for the force on the beam, the stagnation pressure, in [Pa] can be derived from the Bernoulli equation:

$$P = \frac{1}{2}\rho \vec{V}^2 \tag{3}$$

The force F at the center of pressure can then be calculated as:

$$F = PA_{CS} \tag{4}$$

The expected strain at the strain gauge for the cantilever beam can be derived from beam deflection theory; the complete derivation is omitted for clarity. The strain at the strain gauge is given by the following[1]:

$$\epsilon = \frac{6FL}{Ebh^2} \tag{5}$$

where L is the length in [m] from the center of pressure to the center of the strain gauge, E is the elastic modulus of the material in [Pa], b is the width of the beam in [m], and h is the vertical height of the beam in [m]. Note that this assumes a rectangular beam cross section.

2.2. Wheatstone Bridge Theory

Strain gauges consist of a long thin wire of known geometric properties that changes resistance as it is stretched or compressed. If a current is flowing through the strain gauge, this change in resistance directly translates to a change in voltage drop across the strain gauge. Both change in resistance and change in voltage across the gauge can be directly related to the strain by the gauge factor given by the manufacturer. However, because the change in resistance is small, a Wheatstone bridge can be created to detect this change to higher precision, with the strain gauge acting as one of the four resistors. A setup of the Wheatstone Bridge is shown in Figure 2:

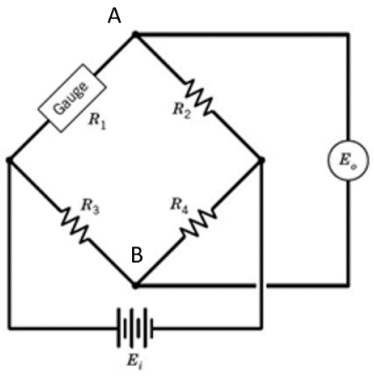

Figure 2: Wheatstone Bridge Schematic (Reproduced from "Strain Gages – Resistance Bridges – Compensation" with permission of the MEMS Dept., University of Pittsburgh)

Initially, the bridge should be balanced to adhere to the zero-voltage output condition when the gauge experiences zero strain. To obtain a balanced bridge, the following equation must hold true:

$$\frac{R_1}{R_3} = \frac{R_2}{R_4} \tag{6}$$

Note that equation (6) can be satisfied by setting all four resistor values to be equal. Additionally, the relationship between change in resistance and the strain at the gauge is given by:

$$\frac{\Delta R}{R} = GF \in_{gauge} \tag{7}$$

Where *GF* is the gauge factor of each strain gauge that is provided by the manufacturer. As the resistance of the strain gauge changes, a measurable potential difference across nodes A and B in Figure 2 results. The following equation can be used to determine the voltage output of the Wheatstone bridge when the gauge is strained:

[1] Equations (1-5) taken from "Detailed Beam Design and Gage Placement Strategy", courtesy of Dr. John Whitefoot and with permission of the MEMS Dept., University of Pittsburgh.

$$\frac{\Delta E_o}{E_i} = \frac{1}{4} GF(\epsilon_1 + \epsilon_2 + \epsilon_3 + \epsilon_4) \quad (8)$$

Where ϵ_1 is the strain of the gauge used in equation (7). The rest of the strains shown in equation (8) are equal to zero, as the remaining resistors in the Wheatstone bridge do not experience a change in resistance.

The bridge constant, κ, must also be considered. Equation (9)[2] demonstrates how to determine the voltage output with the bridge constant considered.

$$\frac{E_o}{E_i} = \frac{1}{4} \kappa GF \epsilon_{gauge} \quad (9)$$

In the case of a quarter bridge, the bridge constant is equal to 1, so the voltage output to voltage input ratio value is unaffected by the inclusion of the bridge constant.

2.3. Signal Conditioning and Calibration

To improve the usability of the voltage signal generated by the change in resistance of the strain gauge, the Wheatstone bridge circuit containing the strain gauge will be connected to both a differential amplifier circuit and an active low-pass filter. This will both amplify the signal to improve the signal measurement, and it will also filter out undesirable frequencies that could produce aliasing in the voltage signal measurement. The circuitry is shown in Figure 3:

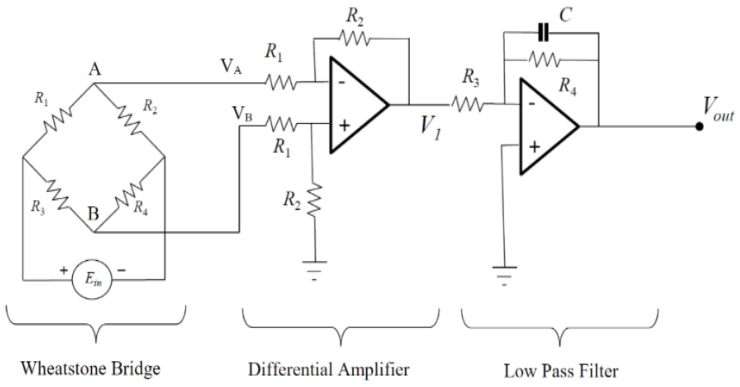

Figure 3: Combined Wheatstone, Differential Amplifier, and Low Pass Filter Circuit, (Reproduced from "MEMS 1041 - Project Circuitry" with permission of the MEMS Dept., University of Pittsburgh)

A differential amplifier is an operational amplifier circuit that is used to amplify the difference between the voltage at the inverting terminal and that of the non-inverting terminal. A basic differential amplifier is shown below in Figure 4:

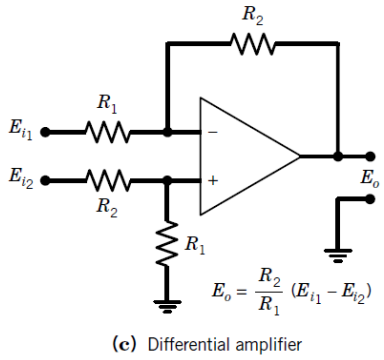

Figure 4: Differential Amplifier Circuit (Reprod. From Theory and Design for Mechanical Measurements, Courtesy of Richard S. Figliola et. al.)

[2] Equations (6-9) taken from "Strain Gages – Resistance Bridges – Compensation" [3] with permission of the MEMS Dept., University of Pittsburgh

The output voltage for a differential amplifier is shown to be

$$E_{o,amp} = V_1 = \frac{R_2}{R_1}(E_{i1} - E_{i2}) = \frac{R_2}{R_1}(V_A - V_B) = \frac{R_2}{R_1}E_{o,bridge} \tag{10}$$

$E_{o,bridge}$ represents the output voltage of the Wheatstone bridge that results from the change in resistance of the strain gauge. The absolute gain for the differential amplifier is

$$G_{amp} = \frac{R_2}{R_1} \tag{11}$$

Once the signal has been amplified by the differential amplifier, it is necessary to filter the signal to ensure there is no aliasing in the signal to improve the accuracy of measurement; if signal aliasing is present, this will directly translate into inaccurate measurements of volumetric flow from the lungs. The filter circuit will thus be constructed to provide approximately 20 [dB] signal reduction, or approximate signal reduction by a factor of 10, at the Nyquist frequency for a given sampling frequency. The Nyquist frequency is given by

$$f_n = \frac{f_s}{2} \tag{12}$$

Where f_s is the sampling frequency. To provide 20 [dB] signal reduction at the Nyquist frequency, the cutoff frequency f_c for the active low-pass filter should be one factor of 10 less than the Nyquist frequency. The formula for the cutoff frequency of the active low-pass filter is given by

$$f_c = \frac{1}{2\pi R_4 C} \tag{13}$$

This filter has a corresponding absolute gain given by[3]

$$G_{filter} = \frac{R_4}{R_3} \tag{14}$$

And thus, the total gain for the amplifier-filter combination is

$$G_{total} = G_{amp}G_{filter} = \frac{R_2 R_4}{R_1 R_3} \tag{15}$$

The gain in [dB] for the circuit is equal to

$$G_{total}\,[dB] = 20\log\left(G_{amp}G_{filter}\right) \tag{16}$$

Note that the above equations reference the resistor values shown in Figure 3. Given the uncertainties and inherent error present in the design and construction of the circuitry and breath force meter apparatus, it is essential to know the exact relationship between applied force at the center of pressure of the breath force meter and measured voltage output. The voltage output is related to the force on the breath force meter by the static sensitivity, a conversion factor in measurement systems that allows for the relation of electrical phenomena to physical phenomena, in this case from units of voltage to units of Newtons.

For the mechanism used for this project, the static sensitivity can be determined by suspending known masses on the plate of the breath force meter at the center of pressure and measuring the change in output voltage of the circuit. The sensitivity of the sensor is given by

$$Sensitivity\ (S) = \frac{Change\ in\ Voltage\ [V]}{Applied\ Force\ [N]} = \frac{\Delta V}{F} \tag{17}$$

Beginning with no mass, the sensor is loaded with increasing mass to generate a plot of output voltage magnitude for a range of samples. The voltage changes for each mass are averaged and the resulting values are plotted against the known applied force values for that mass. The slope of the line of best fit across the points is the static sensitivity value of the sensor. Knowing the value of static sensitivity indicates applied load given a

[3] Equations 10-14 taken from Theory and Design for Mechanical Measurements, Courtesy of Richard S. Figliola et. al.

voltage output, which will be measured by a data acquisition unit. The procedure discusses in further detail how the static sensitivity will further be used to calculate a peak breath force value and the volumetric flow rate from the lungs.

3. Procedure

3.0. Equipment

The following lab equipment was used as part of this experiment:

Table 0: Lab Equipment Used For Experiment

Device	Make and Model Number	Serial Number
Digital Mulitmeter	Rigol DM3058E	DM3R181600608
Function/Arbitrary Waveform Generator	Rigol DG1022	DG1D181401462
Programmable DC Power Supply	Rigol DP832	DP8C181100547
Data Acquisition Unit	National Instruments NI-USB 6008	1E84BED

3.1. Estimating Forces and Relating Forces to Strain Gage Output

Equations (1-5) were combined and used to guide the design of the beam. The beam should produce at least 40 [$\mu strain$] at the gauge for the least forceful breaths and should produce no more than 500 [$\mu strain$] at the gauge for the most forceful breaths. Operating under assumptions and conditions developed in the previous section, the maximum and minimum forces were approximated as

$$F_{max} = 0.1950\ [N]$$

$$F_{min} = 0.04770\ [N]$$

Where F_{max} corresponds to a breath of 7 [L] in 0.9 [s] and F_{min} corresponds to a breath of 5 [L] in 1.3 [s]. A variety of rectangular cross-section beams of varying materials and dimensions were provided in the first laboratory session to be used in the construction of the beam for the breath force meter. Four potential materials were selected to optimize for the desired application, with materials and dimensions summarized in Table 1.

Table 1: Different Beam Materials Considered for Beam Design

Beam Material	Elastic Modulus [GPa][4]	Beam Width [mm]	Beam Thickness [mm]
Stainless Steel	180.	12.77	0.720
Stainless Steel	180.	25.52	0.390
Brass	114.	12.77	0.410
Aluminum	69.0	25.52	0.510

The width and thickness of each material were measured using digital calipers. The aluminum sheet metal was not yet cut to a given width, so a width value equal to that of the second stainless steel beam was adopted for comparison. Additionally, because the beam thickness and width are much harder to manipulate than the length of the beam from the center of pressure to the center of the strain gauge, the length from the center of pressure to the center of the strain gauge was optimized to produce the desirable strain values for a given beam width and thickness specified in the table. Beam lengths from 50.0 [mm] to 200. [mm] were considered, incremented by 5.0 [mm] at a time. Using Equation (5) solved for length in terms of force, elastic modulus, width, and height, values for the strain corresponding to each length for the minimum breath force case were obtained, and the

[4] Values obtained from https://www.engineeringtoolbox.com/young-modulus-d_417.html

results were verified to ensure that the strain for the maximum breath force case did not exceed 500 [$\mu strain$]. See the attached spreadsheet for a more detailed summary of calculations for each beam design.

3.2. Beam Design and Strain Gage Placement

For the first stainless steel beam, the length that produced the closest value to 40 [$\mu strain$] was 165. [mm], corresponding to 39.6 [$\mu strain$]. This beam length is longer than that desired for the breath force meter, so this beam material was removed from consideration. The brass beam produced greater than 40 [$\mu strain$] at the shortest length, and so too was removed from consideration. The aluminum beam produced a value of 40.6 [$\mu strain$] at a length of 65.0 [mm], but this would reduce the mounting area for the bolt, the pressure plate, and the strain gauge with wiring on the beam. Furthermore, the process of cutting the aluminum to-spec would likely damage the material and result in poorer overall quality of results for the project; accordingly, the aluminum was removed from consideration. The second stainless steel beam produced a value of 41.0 [$\mu strain$] at a length of 100.0 [mm]. This allows for a reasonable separation of the mounting bolt, strain gauge, and pressure plate, which improves overall manufacturability. Furthermore, the second stainless steel beam is wider, which should facilitate the mounting of the strain gauge on the surface. The selected design for the breath force meter beam is summarized in Table 2, including strains corresponding to maximum and minimum breath forces.

Table 2: Beam Design Parameters

Beam Parameter	**Value [Units]**
Material	Stainless-steel
Elastic Modulus [GPa]	180.
Length [cm]	10.0
Width [mm]	25.52
Height [mm]	0.390
Minimum Strain [$\mu strain$]	41.0
Maximum Strain [$\mu strain$]	168.

3.3. Mount and Wire Strain Gages to Wheatstone Bridge

Before the strain gauge was mounted, a 5/32” hole was drilled in the selected steel beam approximately 7/16” from the end to allow for the beam to be affixed to the L-bracket of the breath force meter.

Once the hole was drilled, a procedure like that developed by the Vishay Measurements Group in “Strain Gauge Selection Criteria, Procedures, Recommendations” was adopted to mount the strain gauge on the beam. The beam was first treated with Micro-Measurements CSM-3 Degreaser to remove oil, fingerprints, and other imperfections and wiped clean with clean gauze. Throughout the mounting process, a fresh surface of gauze was used for each wipe to prevent contamination of the surface with impurities previously removed. M-PREP Conditioner A was then applied to the beam several times, and the surface was wiped clean. To ensure a more reliable bond between the strain gauge and the beam, the mounting area for the strain gauge was wet sanded with conditioner and 220-grit sandpaper, followed by conditioner and 300-grit sandpaper. The area was sanded until the surface had a uniform appearance, and the area was conditioned and wiped clean with gauze. An X-Acto knife was then used to score a horizontal line across the mounting area where the center of the strain gauge would be placed. Following this, the mounting area was cleaned with M-PREP Neutralizer 5A and cotton swabs until no further residue was visible on the tips of the cotton swab, and then subsequently wiped with fresh gauze.

With the surface prepared for strain gauge mounting, the strain gauge was placed on the mounting area, and cellophane tape was placed over the strain gauge and smoothed with gauze. By peeling the tape back, at a shallow angle of less than 30°, the strain gauge remained affixed to the cellophane tape and was repositioned such that the centerline of the strain gauge was directly over the score mark. After again partially removing the portion of the tape with the strain gauge attached using the procedure described above, the tape was folded back to create a ½" inch margin between the fold in the tape and the bottom of the strain gauge, as shown in Figure 5:

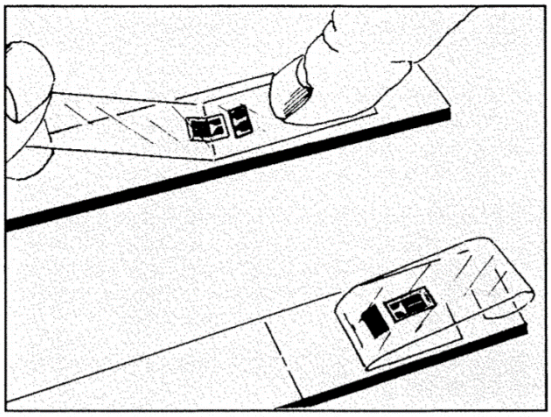

Figure 5: Strain Gauge Mounting Procedure (Reproduced from "Strain Gauge Selection Criteria, Procedures, Recommendations", Courtesy of Vishay Measurements Group

M-BOND 200 Catalyst-C was then brushed onto the mounting surface of the strain gauge sufficient to cover the surface without excess, and two beads of M-BOND 200 Adhesive were then placed at the interface of the beam and the cellophane tape. The cellophane tape was then rapidly folded over and smoothed onto the beam surface using fresh gauze. Firm thumb pressure was then applied directly over the strain gauge for one minute to promote bonding. After allowing the adhesive to cure for five minutes, the cellophane tape was gently folded back directly over itself to separate it from the strain gauge.

Following the mounting of the strain gauge, the strain gauge leads were sanded with 220-grit sandpaper to promote a better solder connection. Two leads of length approximately two feet were subsequently soldered to the strain gauge. The resistance of the strain gauge was then measured using a digital multimeter to be 120.301 [Ω]. Given the pre-drilled hole locations in the L-bracket, it was necessary to adjust the length from the center of the strain gauge to the center of pressure; this new distance was measured using a ruler to be 10.75 [cm], which corresponds to new minimum and maximum strains of 44.0 [$\mu\epsilon$] and 180. [$\mu\epsilon$], respectively (see spreadsheet and equation (5) for calculation).

The leads on the strain gauge were connected to leg 1 of the Wheatstone Bridge shown above. To balance the bridge (using Equation (6)), three 1000 [Ω] potentiometers were adjusted to be as close to 120.301 [Ω] as possible and placed on the other three legs of the Wheatstone bridge. The potentiometer connected to legs 2, 3 and 4 had respective resistances of 120.352 [Ω], 120.336 [Ω], and 120.304 [Ω], respectively. The gauge factor of the strain gauge is known to be 2.14 [-] nominally at 24 [°C], with a 1.2 [%] variation for each [°C] of temperature difference that will be considered negligible for the purposes of this experiment. By applying equations (7) and (8) with zero strain experienced on legs 2,3, and 4 (they are resistors, not strain gauges), a bridge input voltage of 5 [V], and the strains calculated above, the change in resistance of the strain gauge at zero force, the minimum force, and maximum force are:

$$\Delta R_{zero} = 0[\Omega]\,, E_o = 0\ [V]$$

$$\Delta R_{min} = 1.13 \times 10^{-2}\ [\Omega]\,, E_o = 1.18 \times 10^{-4}\ [V]$$

$$\Delta R_{max} = 4.63 \times 10^{-2}\ [\Omega]\,, E_o = 4.82 \times 10^{-4}\ [V]$$

3.4. Amplify and Condition Signal from Strain Gages

To construct the differential amplifier, node A of the Wheatstone bridge was connected to a resistor $R_{1,top}$. The resistor was then connected to a node common to the inverting terminal of a $\mu 741$ operational amplifier and a second resistor $R_{2,top}$. This resistor was then connected to the node at the output of the operational amplifier. Similarly, node B of the Wheatstone bridge was connected to a resistor $R_{1,bottom}$, which was in turn connected to the non-inverting terminal of the operational amplifier and a resistor $R_{2,bottom}$. This resistor was connected to ground on the power supply. Two leads were connected to terminals 4 and 7 of the operational amplifier that will be connected to -15 [V] and +15 [V] on the power supply, respectively. See Figure 3 for reference. The following table is a summary of the resistor values used, the gain of the differential amplifier, and the maximum expected output voltage V_1 of the differential amplifier. Equation (11) was used to calculate the gain of the amplifier using values of $R_{1,top}$ and $R_{2,top}$.

Table 3: Differential Amplifier Circuit Characteristics

$R_{1,top}$ [Ω]	99.630
$R_{1,bottom}$ [Ω]	99.572
$R_{2,top}$ [Ω]	21814
$R_{2,bottom}$ [Ω]	21637
G_{amp} [-]	218.95
$V_{1,max}$ [V]	0.105

To construct the active low pass filter, the V_1 node was connected to a resistor R_3, which was in turn connected to a node common to the inverting terminal of a second $\mu 741$ operational amplifier, a capacitor C, and another resistor R_4. The non-inverting terminal was connected to ground on the power supply, and terminals 4 and 7 received -15 [V] and +15 [V], respectively. The output of the operational amplifier was connected to a node common to the opposite sides of C and R_4; this node carries the output signal voltage V_{out}.

Due to the values of resistors and capacitors available in the measurements lab, the cutoff frequency of the active low-pass filter was limited to those that might be obtained using these combinations. A sampling frequency of 1000 [Hz] was assumed for this experiment such that the Nyquist frequency would be 500 [Hz] by equation (12). The cutoff frequency was thus established to be as close to 50 [Hz] as possible with available values to produce the desired 20 [dB] signal reduction at the Nyquist frequency. Table 4 summarizes the results of the iterative study and the characteristics of the active low-pass filter. Equations (11) and (13) were used to calculate the gain and cutoff frequency, respectively. See attached Excel sheet for detailed calculations of cutoff frequencies for available resistor and capacitor values.

Table 4: Active Low-Pass Filter Circuit Characteristics

R_3 [Ω]	197.0
R_4 [Ω]	4625.
C [μF]	0.6850
f_c [Hz]	50.24
G_{filter} [-]	23.48

The total gain for the circuit is given by equations (15) and (16) as

$$G_{total} = 5140.[-] = 74.22\ [dB]$$

The maximum V_{out} occurs when the strain is maximized. Using the output voltage values derived previously for the maximum and minimum cases, along with equation (15) and the total gain, the upper and lower bounds of output voltage are

$$V_{out,min} = 0\ [V]$$

$$V_{out,max} = 2.48[V]$$

Due to discrepancies in resistor values for the Wheatstone bridge and differential amplifier circuits, the minimum output voltage will be small, but nonzero. This will be addressed by calibrating the circuitry.

Before the breath force meter was calibrated, tests were conducted on each portion of the signal conditioning circuitry to ensure their respective functions. For the Wheatstone bridge, 5[V] DC voltage was sent to the input of the bridge, and the potential difference across nodes A and B, denoted as $V_A - V_B$, was measured. Under a truly balanced condition, the potential difference $V_A - V_B$ would be zero; the actual potential difference was observed to be -3.13 [mV]. A target of less than 5 [mV] was sought, and so the Wheatstone bridge output was determined to be satisfactory. Additionally, when the beam was placed under a load, the output voltage fluctuated by about 1 [mV], and so there was a demonstrable response of the Wheatstone bridge to the strain of the strain gauge.

For the differential amplifier, the operational amplifier was powered with $\pm 15\ [V]$ from the power supply. A signal of 10 [mV], RMS was sent from the function generator to the amplifier, with the positive terminal on the power supply connected to V_A and the negative terminal connected to V_B. The signal at the output of the differential amplifier was measured using the digital multimeter, and the actual absolute gain was observed to be approximately 225.6 [-].

For the active low-pass filter, the operational amplifier was powered with $\pm 15\ [V]$ from the power supply. A 10 [mV] RMS signal with frequency 15 [Hz] was sent to V_1 and into the filter. The gain was observed to be 23.9 [-] at this frequency, compared to 23.5 [-] expected. The frequency was then incrementally increased to 50 [Hz] (the theoretical cutoff frequency), where the gain was observed to be 11.5, corresponding to a -2.72 [dB] reduction in magnitude from that observed at 15 [Hz]. The signal magnitude continually decreased above 50 [Hz].

3.5. Sensor Calibration

Once the functionality of the circuitry was validated, the sensor was calibrated by suspending known masses from the breath force meter and recording the change in output voltage. The breath force meter was affixed to the lab bench such that the beam was horizontally oriented, as shown in Figure 6.

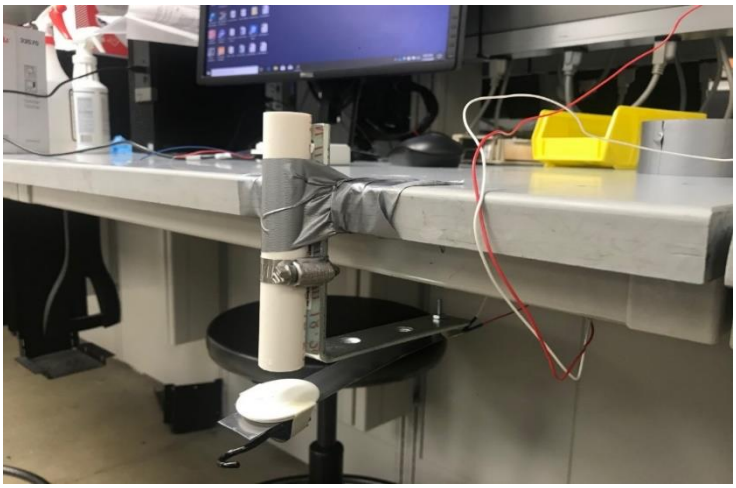

Figure 6: Configuration of Breath Force Meter for Calibration

The output of the low-pass filter was connected to a NI USB-6008 Data Acquisition Unit, and the data acquisition script from Lab 1 was modified to suit this experiment (See Appendix A). The voltage difference due to the beam's own weight and due to separate applied masses of 10, 20, and 30 grams were recorded and plotted vs. sample number. The voltage output was recorded for each of the suspended masses with the beam initially supported by hand to remove strain from the gauge, and then the beam could come to equilibrium under the influence of the masses.

3.6. Measuring Breath Force

After calibration was complete, the breath force meter was detached from the table and the beam was aligned vertically to remove the effect of the beam's own weight on the breath measurements. At the end of the tube furthest from the beam, a hand pump with a capacity of 1.70 [L] was connected to the breath force meter. The testing setup is shown below in Figure 7.

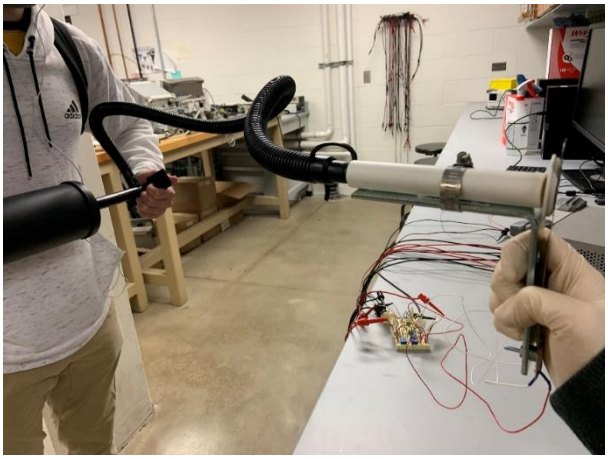

Figure 7: Breath Force Meter Test Setup

The data acquisition unit was connected to the output of the low-pass filter to take voltage measurements, and the hand pump was discharged to model an exhale in which the air was delivered to the plate. The beam deflected as a result and generated a voltage reading that was then recorded and plotted. The beam deflection can be shown below in Figure 8.

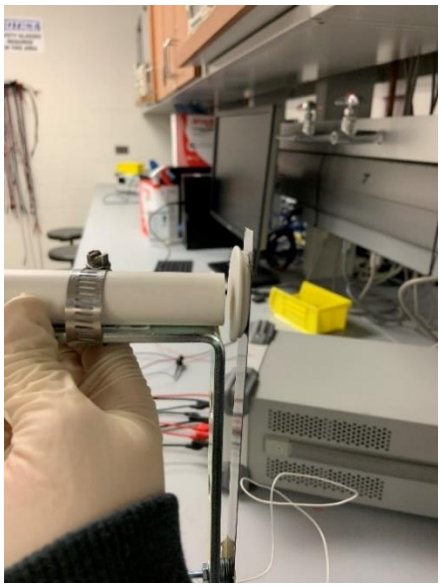

Figure 8: Breath Force Meter Beam Deflection

This process was repeated for a total of ten trials, of which five were selected for further analysis.

4. Summary of Results

Figure 9 shows a sample response of the measurement system to a suspended mass of 20 grams during the calibration of the sensor.

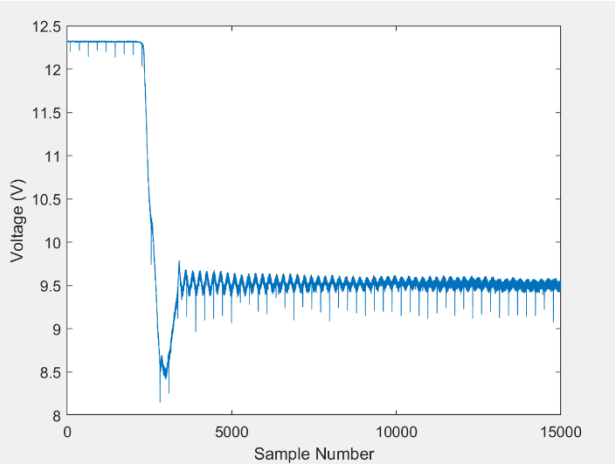

Figure 9: Voltage Response of Measurement System to 20-gram Mass Supported at Center of Pressure

The unloaded state compared to the loaded state can be clearly discerned from the change in voltage at an approximate sample number of 3000 in the above example. The average value of voltage across the unloaded state sample range and the loaded state sample range were computed in MATLAB for each mass, and the magnitude of the average change in voltage was computed. Note that the large initial voltage value is due to the nonzero output of the Wheatstone bridge before amplification, and the measured voltage decreases because the strain gauge is in compression on the beam. The results are summarized in Table 5 and Figure 10.

Table 5: Change in Output Voltage for Known Applied Forces

Applied Force [N]	Change in Output Voltage [V]
0	-1
0.0981	-2.43
0.1962	-3.67
0.2943	-6.08

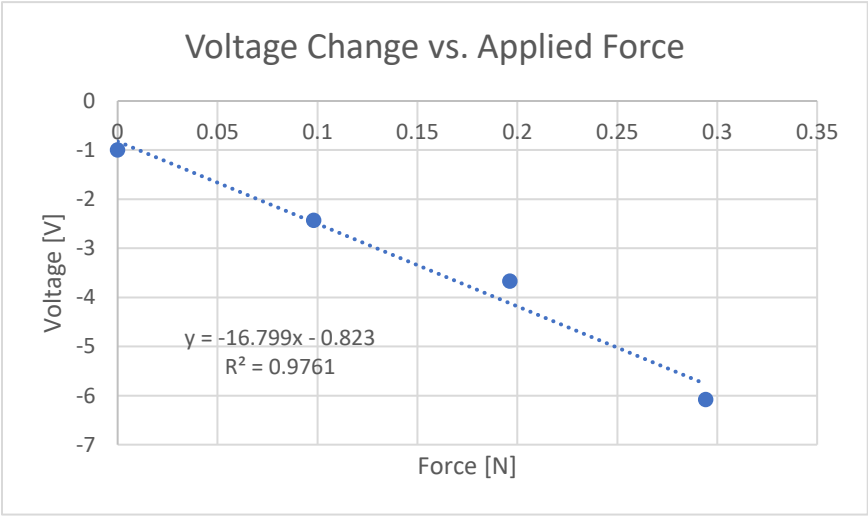

Figure 10: Change in Output Voltage vs. Applied Force

From a plot of the data, the slope of the best-fit trendline was calculated to be -16.8 [V/N], representing the static sensitivity of the sensor, with a correlation coefficient of 0.9761. Thus, the change in output voltage relative to the initial measured voltage can be used to determine the force on the beam, which in turn can be used to determine the average and peak breath force, along with the volumetric capacity of the lungs.

Following the trials, a plot of change in voltage (magnitude) vs. sample number was examined to ascertain the approximate range of samples for which the volume of the pump was dispensed. A Butterworth filter with cutoff frequency of 200 [Hz] was applied to the data, and ”movmedian” MATLAB function was used to eliminate outliers in data resulting from noise. Figure 11 shows one such plot:

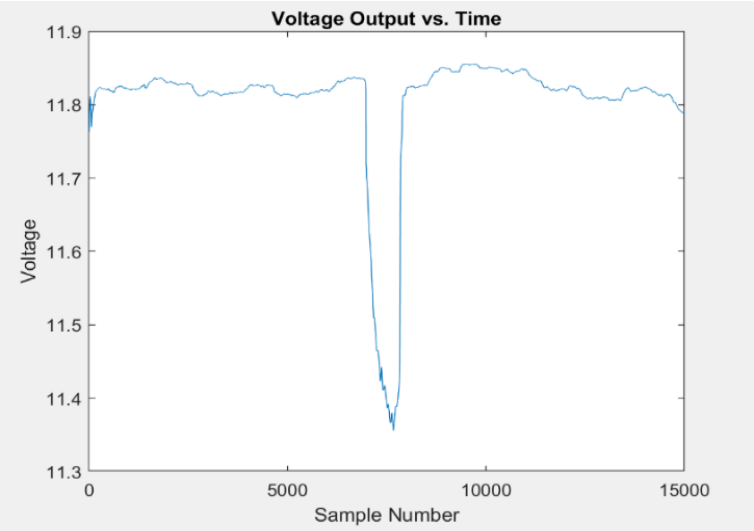

Figure 11: Change in Voltage for Pump Test

From this plot, the approximate range of samples for the pump volume dispensation was approximated. Over this range, the voltage output magnitude relative to the average voltage output under no strain was calculated. The results for all five trials are shown in Figure 12.

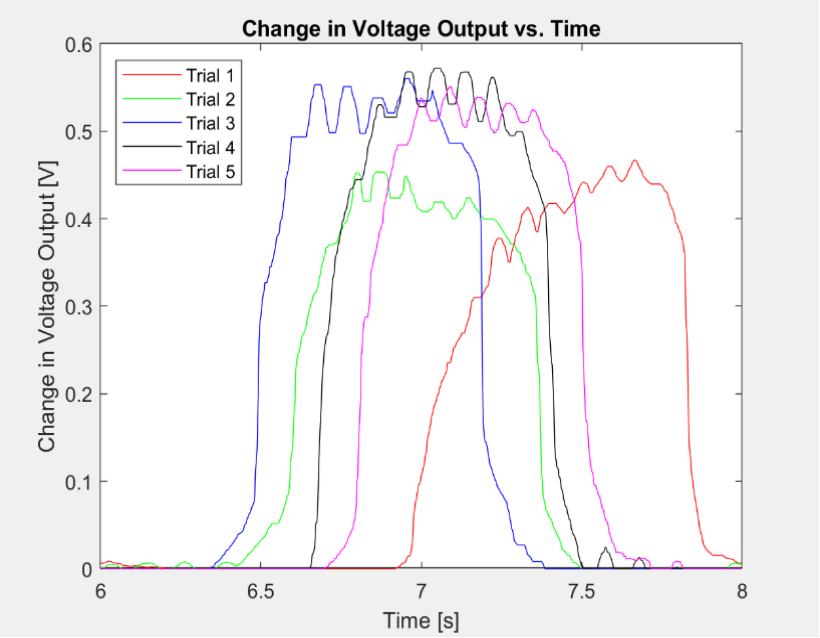

Figure 12: Change in Voltage for Pump Test

Note that equations (2-4) and (17) can be combined to yield

$$\dot{V} = \sqrt{\frac{2\Delta V A_{CS}}{\rho S}} \tag{18}$$

Where $\dot{V}$ is the volumetric flowrate, ΔV is the magnitude of change in voltage with respect to the initial value for the trial, and S is the sensitivity of the breath force meter. By integrating this equation with respect to time over the duration of the breath, the volumetric capacity of the pump/lungs can be determined. A Riemann sum approximation was used to do so. Furthermore, the peak breath force is the maximum voltage change magnitude value divided by the sensitivity of the sensor, and average breath force is the average change in voltage magnitude divided by the sensitivity of the sensor. Equation (7) was used to calculate the maximum strain experienced by the beam from the peak force values.

Table 5 summarizes the volumetric flow, peak breath force, average breath force, and peak strain for each of the five trials.

Table 5: Measured Volumetric Flow, Peak Breath Force, and Average Breath Force

Trial	Volumetric Flow [L]	Peak Breath Force [N]	Average Breath Force [N]	Peak Strain [μs]
1	2.39	0.0278	0.0191	25.7
2	2.39	0.0270	0.0178	24.9
3	2.40	0.0333	0.0215	30.8
4	2.34	0.0340	0.0255	31.5
5	2.34	0.0328	0.0227	30.3
Average	2.37	0.0310	0.0213	28.6
St. Dev.	0.0295 (1.24 [%])	0.0033 (10.6 [%])	0.0031 (14.6 [%])	3.09 (10.7 [%])

5. Discussion

5.1. Comparing to Theory in Calibration

During calibration, the observed strain (and by direct association the output voltage of the circuit) were greater than that expected for each of the known masses after removing the effect of the beam's own weight. Equations (5), (8), and (15) were combined to obtain an expected output voltage for each of the known masses. The difference between this value and the actual measured output was back-substituted into these equations to calculate a difference in measured vs. expected strain. Table 6 summarizes the results of this analysis.

Table 6: Measured Volumetric Flow, Peak Breath Force, and Average Breath Force

Suspended Weight [N]	Expected Strain [μs]	Observed Strain [μs]	Percent Error [%]
0.0981	90.6	104.6	+15.4
0.1962	181.	193.	+6.63
0.2943	272.	370.	+36.0

The values were significantly greater for each suspended mass than the theoretical value, particularly in the case of the largest suspended mass. This may result from the breakdown of beam deflection theory assumptions, particularly the fact that the deflection of the beam is assumed to be very small relative to the length of the beam; for the 0.2943 [N] load, the beam deflected a considerable amount. Additional minor error may also be introduced by errors in measurement of the physical properties of the beam. Additionally, the differences in measured and expected strain may be partially due to uncertainty in the measurement of the electrical properties of the circuitry; the op amps used were not balanced at the offset terminals, which may induce non-ideal

behavior. The end result is inaccuracy in the determination of static sensitivity, which propagated through to the measurement of volumetric flow and force characteristics.

5.2. Comparison of Forces and Volumetric Flow to Expected Range of Inputs

Even with calibration, the measured values for volumetric flow, peak breath force, and peak strain were significantly different than those expected in theory. On average, the measured volumetric flow for the pump was 0.67 [L] greater than the nominal capacity of 1.70 [L], representing a 40% overestimation of lung capacity. Several possibilities exist as sources of error that could have resulted in a greater measured lung capacity. For instance, because the beam was held in the hand while the volume of the pump was dispensed, there could have been inadvertent contributions to the deflection of the beam resulting from the beam's weight if it was not oriented perfectly horizontally. Furthermore, variation in material properties (i.e., elastic modulus) resulting from imperfections and measurement error of the beam itself may have resulted in inaccurate representations of the beam's properties that carried through to calculations of total volumetric flow. Barring error in the electrical circuitry, the calibration of the sensor to determine its sensitivity should have been sufficient to relate force to voltage output, which directly translates to volumetric flow. However, the regression line for calibration was not perfect, due to sources of uncertainty described above, and so the sensitivity of the breath force meter may vary from that used for the experiment.

Regarding the forces and strains, both were consistently significantly less than what was expected based on preliminary calculations. One significant reason for this is the difference in volume between the pump and the theoretical capacity of the human lungs. The minimum expected strain figured on an exhaled volume of 5 [L] in approximately 1 second; for testing, the exhaled volume was under 40 percent of this amount in a comparable timeframe. Also note that the combination of equations (2-4) implies that the force experienced by the beam has a square dependence on the volume flowrate, which magnifies its effect on the experimentally determined forces and strains. Another source of error in the measurement of the breath force results from non-laminar flow of the air once the beam has deflected to a certain degree. The result is eddy losses once the air has left the end of the PVC tube but before it meets the pressure plate. These losses result in significant reduction in velocity of the air in this gap, which increase with its width; this explains the oscillatory behavior of the voltage signal at the peaks of the data. As the beam deflects more, more losses occur that result in less force on the beam. The beam thus deflects less and experiences a corresponding increase in force as less losses occur. The result is that the peak force in theory is higher because the stagnation pressure assumes laminar flow throughout the trial. There are secondary errors introduced by assumptions of the properties of the air, beam properties, and voltage measurement as described above. The conjunction of these with eddy losses and volumetric differences together likely account for the deviation of peak force and peak strain from the theoretical values.

The volumetric flow measurement was fairly repeatable, with a standard deviation of 1.3 [%] from the average measured volumetric flow value. However, the results were not necessarily accurate, as discussed previously. Measurement of peak force, average force, and peak strain were more variable, with standard deviations of 10.6 [%], 14.6 [%], and 10.7 [%], respectively. The variation in these parameters may result more so from the testing procedure than from measurement error, as the volume flowrate that determines these parameters varied from trial to trial due to variation in the rapidity with which the plunger was depressed on the pump by its operator.

Although the breath force meter measures total volumetric flow with a relatively high degree of precision, its accuracy is not satisfactory. If this device is being used to indicate whether the volume within the lungs is below accepted amounts, this device would overestimate it, which is not ideal. To remove the confounding effect of the plunger operation procedure, we recommend fixing the geometry of the pump such that the applied force to the pump remains constant throughout the trial. This may take the form of fixing masses to the plunger and orienting the pump vertically such that the effect of the attached masses fully dispenses the volume of the pump in a more repeatable fashion. It would be more meaningful to measure the volume flowrate from the pump under these conditions in advance so that results of the testing can be more directly compared to what is expected initially. For instance, if it is known that the full volume of 1.70 [L] is dispensed over a period of 1.2 [s], this information could be used to better approximate the strains and forces on the beam to facilitate design. Furthermore, the experimental peak strain and peak force would be able to be directly compared to what is

expected in theory. The eddy losses in the airflow can be mitigated by designing a shorter beam; because the beam is shorter, it will deflect less assuming that the cross-sectional properties and applied force remain constant. This reduces the gap between the pressure plate and the end of the PVC tube in which the losses take place, and the laminar flow assumption would be more accurate. The expected result would be a reduction in the oscillatory behavior of the beam at the peak of the change in voltage vs. time curve. Additionally, it was difficult to accurately measure the length from the center of the strain gauge to the center of pressure on the plate. In a future experiment, better accuracy may be obtained in this measurement by marking the center of pressure on the beam before applying the plate. Regarding the circuitry, a potentiometer could be employed for both the differential amplifier and filter circuits to ensure that the output voltage is zero when the op amp is only being powered.

6. References:

[1] Whitefoot, John. “Detailed Beam Design and Gage Placement Strategy.” 2020.

[2] Whitefoot, John. “MEMS 1041 Semester Project Description.” 2020.

[3] Whitefoot, John. “Strain Gages – Resistance Bridges – Compensation.” 2020.

[4] Whitefoot, John. “MEMS 1041 – Project Circuitry”. 2020.

[5] Figliola, Richard S., and Donald E. Beasley. *Theory and Design for Mechanical Measurements.* 5th ed., John Wiley & Sons, 2011.

[6] “Strain Gauge Selection Criteria, Procedures, Recommendations.” Vishay Measurements Group, 30 May 2018.

[7] Whitefoot, John “Calibration and Data Acquisition”. 2020

7. Appendix A:

Matlab Data Acquisition Code with modified record time, channel range, and data plotting used for this lab from the MEMS 1041 Lab #1 Module. Created by and reproduced with permission from Dr. John Whitefoot, MEMS Department, University of Pittsburgh.

```
clear all % clears the workspace
close all % closes all open figures

filename = 'test_data_30_1gram'; % file name for saving data in a Matlab .mat file_1

fs=1000;        % sampling frequency (Hz)
record_time=15;  % amount of time to record data (sec)

% Create a DAQ session within Matlab to look for the NI (National
% Instruments) DAQ

s=daq.createSession('ni');

% Tell Matlab to use one analog input channel from device number 'devX'
% NOTE: you'll have to update the device number depending on what is
% assigned when you connect the DAQ to the computer

[ch,idx]=s.addAnalogInputChannel('dev2','ai0','Voltage');

% specify the voltage range of the channel. If your range is too small
% your data peaks will be "clipped" at the maximum/minimum values you
% specify

ch(1).Range=[-15 15];

% set the sampling frequency (fs) and duration of the recording
% (record_time)

s.Rate=fs;
s.DurationInSeconds=record_time;

% We must first create a listener to allow us to look at the data
% mid-stream and make sure there is data in the first place. In order
% to do this, we will first need to add the following "listener"

listen=s.addlistener('DataAvailable',@(s,event) plot(event.TimeStamps,event.Data));

% start data capture, where "data" is the recorded voltage signal and "t" is the time in
% seconds
[data,t]=s.startForeground();

sampleno=fs.*t;

% plot your final data vs. time
plot(sampleno,data); xlabel('Sample Number'); ylabel('Voltage (V)');

% save a copy of the plot
saveas(gcf,filename,'fig');

% save your data as a .mat file so you can load it into Matlab later using
% the load() command
save(filename);
```